The Astrophysical Journal, 767:172 (15pp), 2013 April 20 doi:10.1088/0004-637X/767/2/172

JOVIAN STRATOSPHERE AS A CHEMICAL TRANSPORT SYSTEM: BENCHMARK ANALYTICAL SOLUTIONS

Xi Zhang, Run-Lie Shia, and Yuk L. Yung
Division of Geological and Planetary Sciences, California Institute of Technology, Pasadena, CA 91125, USA; xiz@gps.caltech.edu
Received 2013 January 2; accepted 2013 March 7; published 2013 April 8

ABSTRACT

We systematically investigated the solvable analytical benchmark cases in both one- and two-dimensional (1D and 2D) chemical–advective–diffusive systems. We use the stratosphere of Jupiter as an example but the results can be applied to other planetary atmospheres and exoplanetary atmospheres. In the 1D system, we show that CH_4 and C_2H_6 are mainly in diffusive equilibrium, and the C_2H_2 profile can be approximated by modified Bessel functions. In the 2D system in the meridional plane, analytical solutions for two typical circulation patterns are derived. Simple tracer transport modeling demonstrates that the distribution of a short-lived species (such as C_2H_2) is dominated by the local chemical sources and sinks, while that of a long-lived species (such as C_2H_6) is significantly influenced by the circulation pattern. We find that an equator-to-pole circulation could qualitatively explain the *Cassini* observations, but a pure diffusive transport process could not. For slowly rotating planets like the close-in extrasolar planets, the interaction between the advection by the zonal wind and chemistry might cause a phase lag between the final tracer distribution and the original source distribution. The numerical simulation results from the 2D Caltech/JPL chemistry-transport model agree well with the analytical solutions for various cases.

Key words: astrochemistry – methods: analytical – planets and satellites: atmospheres – planets and satellites: individual (exo-planets, Jupiter)

Online-only material: color figures

1. INTRODUCTION

The Jovian stratosphere is an ideal laboratory for the study of atmospheric tracer transport. The stratosphere is dominated by hydrocarbon photochemistry, driven by the photolysis of the parent species, methane (CH_4), which is transported from the deep atmosphere. The two most abundant photochemical products, acetylene (C_2H_2) and ethane (C_2H_6), have properties that make them ideal tracers. First, apart from CH_4, they show the most prominent features in the middle infrared emission spectra of Jupiter. Therefore, their latitudinal and vertical distributions can be accurately determined. Second, their chemical lifetimes differ widely, ranging from several Earth years (C_2H_2) to several hundreds of Earth years (C_2H_6). That means they have different sensitivity to the transport. In fact, their latitudinal profiles (Nixon et al. 2007) show opposite trends, implying that the transport timescale is probably located between the two lifetimes. Third, their chemistry is relatively simple and most of the chemical reaction coefficients have been measured in the laboratory with small uncertainties. Unlike the other possible tracers, such as hydrogen cyanide (HCN) and carbon dioxide (CO_2), whose vertical distribution is not known (Lellouch et al. 2006), or aerosol, which might be affected by complicated microphysics, the simple pair C_2H_2 and C_2H_6 provides a wealth of information on the stratospheric circulation on Jupiter.

Most of the previous studies focused on 1D chemistry-diffusion models (e.g., Strobel 1974; Gladstone et al. 1996; Moses et al. 2005), which essentially ignore the latitudinal transport. The advantages of a 1D model are: (1) it is numerically stable due to the nature of diffusive processes; (2) the computation is usually fast, and therefore it can include a very complicated network of chemical reactions (Moses et al. 2005). Once the horizontal and vertical advection terms are added, the model is subject to numerical instability and limited by the Courant–Friedrichs–Lewy (CFL) criterion, although the 2D calculation is more realistic.

There is no definitive 2D chemistry-transport model (CTM) for the stratosphere of Jupiter, taking into account the photochemistry, eddy and molecular diffusion, and the vertical and horizontal advection, although the existence of large-scale stratospheric circulation has been hypothesized since the 1990s (e.g., Conrath et al. 1990; West et al. 1992). Friedson et al. (1999) proposed that horizontal eddy mixing processes dominate the transport of the SL9 debris in the stratosphere of Jupiter. Liang et al. (2005) used a 2D chemistry-diffusion model and found that the horizontal mixing might be enough to explain the latitudinal profiles of C_2H_2 and C_2H_6. A simple 1D model in the latitudinal coordinate by Lellouch et al. (2006) shows that the dynamical pictures derived from HCN and CO_2 are not consistent with each other, and also not with the C_2H_2 and C_2H_6 profiles. Both Liang et al. (2005) and Lellouch et al. (2006) suggested that the *horizontal* eddy diffusivity is required to vary with latitude and altitude, leading to a more complicated picture. Note that the C_2H_6 distribution cited in their studies decreases from low latitudes to high latitudes. The recent analysis of *Cassini* and *Voyager* spectra has revealed more accurate latitudinal profiles of C_2H_6 (Nixon et al. 2010; Zhang et al. 2013), which are clearly enhanced in the high latitudes, especially in the *Voyager* era. One might also use a latitudinally varying *vertical* eddy diffusivity profile to explain the C_2H_6 *horizontal* distribution via changing its *vertical* slope with latitude (Lellouch et al. 2006). However, this approach might be no different from a parameterization of a realistic horizontal and vertical advection process. Instead, a full CTM is needed to understand the tracer transport in the stratosphere of Jupiter.

As mentioned above, a very careful treatment of the numerical scheme is necessary in the CTM since the advection terms might lead to inaccurate results. Shia et al. (1990) compared different numerical schemes and adopted the modified Prather scheme

(Prather 1986) in the Caltech/JPL Kinetics CTM. In that paper, the authors derived several analytical solutions to validate the numerical results, in both 1D and 2D. But the authors only used the analytic solutions to test the numerical scheme and did not discuss the underlying physical implications of those analytical results. Therefore, some of their analytical results were mathematically correct but physically counterintuitive (such as a negative chemical production rate).

On the other hand, the nonlinear feedbacks in the complicated chemical–advective–diffusive system may blur the physical insights. A simple but realistic analytical solution can be considered as a benchmark case for understanding the basic behavior of the system, under idealized assumptions. Previous studies did not focus on analytical benchmark cases in atmospheric tracer transport. In civil engineering, the regional Gaussian-plume dispersion models have been studied for many years, and the analytical solutions for the three-dimensional (3D) diffusion equation could be obtained, although they may not be in explicit form (e.g., Lin & Hildemann 1997). But those solutions are not useful for this study because (1) they are too complicated to foster any physical insight, (2) they are restricted to a nonreactive contaminant, and (3) they are not on the planetary scale in which the sphericity of the planet should be taken into account. For the simple planetary-scale analytical solutions, apart from Shia et al. (1990), previous attempts focused mainly on the 1D solutions. Neglecting the chemistry, Chamberlain & Hunten (1987) derived a 1D analytical solution with an exponential form of eddy and molecular diffusivities. Yelle et al. (2001) reported a 1D diffusive equilibrium CH_4 profile, which is essentially a special case of that found by Chamberlain & Hunten (1987). A systematic study of the available analytical cases in the planetary chemical-transport system has been lacking.

In this study, we systematically investigate the behavior of the chemical–advective–diffusive system through various representative analytical benchmark cases, such as for the long-lived species versus the short-lived species. Those analytical formulae will be used to validate the numerical simulations in which the numerical schemes are not trivial. We will focus on hydrocarbons in the stratosphere of Jupiter because the observations of C_2H_2 and C_2H_6 show a beautiful example of the tracer transport systems. In order to derive the analytical formulae, we need to make some simplifying assumptions; therefore, we will leave to a future study the detailed numerical modeling with realistic hydrocarbon chemistry and circulation pattern inferred from radiative modeling (Zhang 2012; Zhang et al. 2013). Finally, our results could be applied to other planetary and exoplanetary atmospheres.

This paper is structured as follows. In Section 2, we will introduce the chemical–advective–diffusive equation. In Section 3, we will solve the equation in the 1D system. In Sections 4 and 5, we will focus on the 2D systems in the meridional plane and zonal plane, respectively, followed by a summary in Section 6.

2. THE NATURE OF THE PROBLEM

Let us first consider a chemical system in a fast-rotating atmosphere. Every quantity can be zonally averaged. We adopt the transformed Eulerian mean (TEM) formulation (Andrews et al. 1987, hereafter AHL1987) here. Chemical species are transported vertically and meridionally by the *residual mean circulation* driven by the diabatic circulation, with a vertical effective transport velocity w and a meridional effective transport velocity v. We also parameterize the eddy transport in a "diffusion" tensor that governs the tracer mixing processes both vertically and meridionally (see AHL1987, p. 354). In the region above the homopause, species of different mass would separate from each other by molecular diffusion.

We adopt a vertical coordinate $z = H\ \ln(p_s/p)$, where p is pressure and p_s is the reference pressure, which is usually taken to be 1 bar for giant planets. H is the pressure scale height of the background atmosphere. The meridional coordinate is $y = a\theta$, where a is planetary radius and θ is the latitude. We further define a dimensionless coordinate $\xi = z/H$. The volume mixing ratio of gas (or tracer) i is $\chi = N_i/N$, where N_i and N are the concentrations of gas and background atmosphere, respectively. Below the homopause, the full form of the zonal-averaged Eulerian mean transport equation for a 2D chemical system is (Shia et al. 1990)

$$\frac{\partial \chi}{\partial t} + v\frac{\partial \chi}{\partial y} + w\frac{\partial \chi}{\partial z} - \frac{1}{\cos\theta}\frac{\partial}{\partial y}\left(\cos\theta K_{yy}\frac{\partial \chi}{\partial y}\right) - e^{\xi}\frac{\partial}{\partial z}\left(e^{-\xi}K_{zz}\frac{\partial \chi}{\partial z}\right) = \frac{P-L}{N}, \quad (1)$$

where P and L are the chemical source and loss terms, respectively. Here we use only the diagonal term of the diffusion tensor K. This is an advantage of the TEM formulation: since the diabatic circulation has already taken into account the y–z-direction transport, we can neglect the K_{yz} and K_{zy} terms (AHL1987, p. 380). Above the homopause, strictly speaking, we should also consider molecular diffusion. However, the transport by the residual circulation is usually more effective in the region where eddy mixing dominates, so we neglect it above the homopause in the 2D systems. We will consider molecular diffusion in the 1D system (Section 3).

For the numerical simulation, we use the Caltech/JPL kinetics model. The 1D model is taken from the state-of-the-art chemical schemes for the Jovian stratosphere from Moses et al. (2005). The model integrates the continuity equation including chemistry and vertical diffusion using a matrix inversion method (Allen et al. 1981). For the 2D simulations in the meridional plane, we adopt the numerical model from Shia et al. (1990) for a single tracer. The details will be discussed in Section 4.

3. 1D SYSTEM

Consider a 1D chemical-transport system in the vertical coordinate in the global-average sense. Above the homopause, the vertical diffusive flux $\phi_z = NK_{zz}\partial\chi/\partial z$ needs to be modified to include molecular diffusion

$$\phi_z = NK_{zz}\frac{\partial \chi}{\partial z} + ND_i\frac{\partial(N_i/N_{eq,i})}{\partial z}, \quad (2)$$

where D_i is the molecular diffusivity for gas component i in the background atmosphere, $N_{eq,i}$ is the equilibrium density profile with the scale height of species i. After some manipulation, the continuity equation becomes

$$\frac{\partial \chi}{\partial t} + w\frac{\partial \chi}{\partial z} - e^{\xi}\frac{\partial}{\partial z}\left\{e^{-\xi}\left[(K_{zz}+D_i)\frac{\partial \chi}{\partial z} + \frac{fD_i}{H}\chi\right]\right\} = \frac{P-L}{N}. \quad (3)$$

where $f = m_i/m - 1$, m_i and m are the molecular mass of the species i and the background atmosphere, respectively. In order to derive analytical solutions, we assume specific forms for eddy diffusivity and molecular diffusivity. Lindzen (1981) proposed a wave-breaking turbulent mixing diffusivity, which satisfies $K_{zz} \propto N^{-1/2}$. The binary molecular diffusion theory

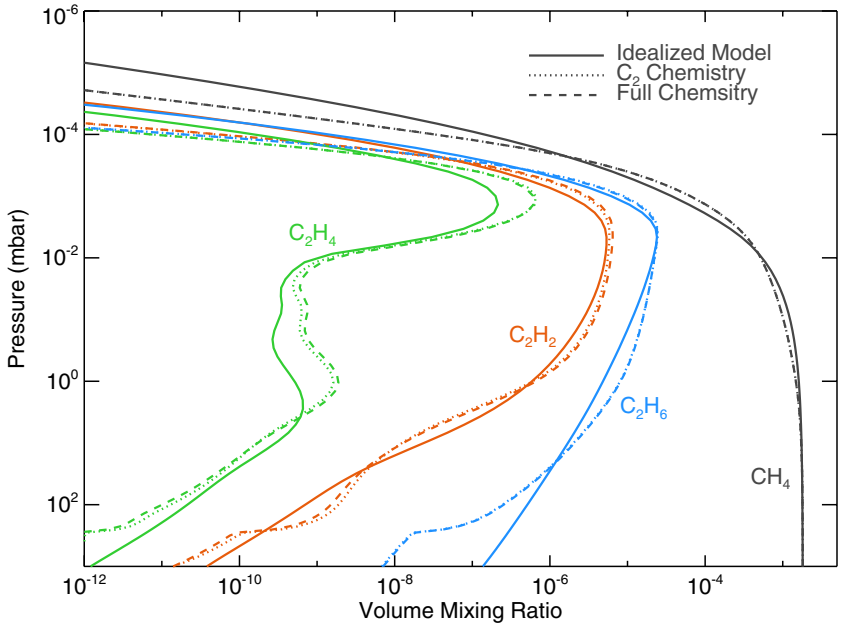

Figure 1. Simulated hydrocarbon profiles from the idealized model, the C_2 chemistry model (with realistic eddy and molecular diffusivities as in the full chemistry model) and the full chemistry model.

(A color version of this figure is available in the online journal.)

implies $D_i \propto N^{-1}$ (Chamberlain & Hunten 1987). In this study we assume $K_{zz} = K_0 e^{\gamma\xi}$ and $D_i = D_0 e^{\xi}$.

For an isothermal atmosphere which approximates the Jovian stratosphere, we have $N = N_0 e^{-\xi}$. For the chemical production and loss terms, we assume $P = P_0 N_0 e^{\alpha\xi}$, and $L = L_0 N e^{\beta\xi}\chi = L_0 N_0 e^{(\beta-1)\xi}\chi$. For a nondivergent flow we take $w = w_0 e^{\xi} \propto N^{-1}$. For steady state with $\partial\chi/\partial t = 0$ in the vertical coordinate ξ, Equation (3) becomes

$$[D_0 + K_0 e^{(\gamma-1)\xi}]\frac{d^2\chi}{d\xi^2} + [f D_0 - w_0 H + K_0(\gamma-1)e^{(\gamma-1)\xi}]\frac{d\chi}{d\xi} - L_0 H^2 e^{(\beta-1)\xi}\chi + P_0 H^2 e^{\alpha\xi} = 0. \quad (4)$$

Equation (4) is the governing equation for the 1D chemical–advective–diffusive system. There is no general solution for this equation except under some specific conditions. If $\gamma = \beta = 1$, we could obtain an analytical solution by following the derivation of Shia et al. (1990). If $\beta = 1$ and $P_0 = 0$, there could be a solution expressed by the hypergeometric functions. Alternatively, we consider the cases with $\gamma \sim 0.5$, which are based on Lindzen's hypothesis and also approximate the situation in the Jovian stratosphere (Moses et al. 2005).

We simplify the Moses et al. (2005) model to an idealized model by assuming an isothermal atmosphere and using simplified molecular and eddy diffusivity profiles, with the chemistry including only the C_2 hydrocarbons. The results from the idealized model are very close to those from the full chemistry model. Figure 1 shows the numerical results compared with the full chemistry model from Moses et al. (2005), a reduced C_2 chemistry model with realistic chemistry and diffusivity, and our idealized model. The simplified eddy diffusivity and molecular diffusivity are shown in Figure 2. For Jupiter, we take $T_0 = 150$ K, $H = 24.1$ km, $K_0 \sim 280\,\mathrm{cm^2\,s^{-1}}$, and $D_0 \sim 0.04\,\mathrm{cm^2\,s^{-1}}$ for CH_4 and $0.03\,\mathrm{cm^2\,s^{-1}}$ for C_2H_2 and C_2H_6 (scaled by the square root of molecular mass).

In principle, it is not proper to include vertical wind in the 1D model because it will go to infinity when the atmospheric density drops to zero at the top boundary. However, if we artificially add wind in the 1D case, it is also useful to roughly estimate the effect of vertical transport in the 2D case. Therefore, we derived the solutions for both wind-free ($w_0 = 0$) and wind cases ($w_0 \neq 0$). The solutions of the 1D chemical system are summarized in Table 1. The detailed derivations can be found in Zhang (2012, chap. V).

3.1. Cases without Wind

If we set $w_0 = 0$, three typical cases are used to explain the distributions of CH_4, C_2H_6, and C_2H_2 in the Jovian stratosphere.

3.1.1. CH_4

CH_4 is transported upward from the interior. If we neglect photolysis, CH_4 will be governed by the diffusion equilibrium, corresponding to case I in Table 1. This is generally true because the strong self-shielding effect will limit its photolysis efficiency below some pressure level. From Moses et al. (2005), the upward flux, F, is on the order of $10^9\,\mathrm{cm^2\,s^{-1}}$, so FH/fN_0D_0 is $\sim 10^{-5}$ in the solution of case I. Compared with the CH_4 mixing ratio in the deep interior, determined by the thermochemistry ($\chi_0 \sim 1.8 \times 10^{-3}$), the flux term can be ignored. With the above assumptions, the solution of case I is

$$\chi(\xi) = \chi_0 \left(\frac{D_0 e^{(1-\gamma)\xi} + K_0}{D_0 + K_0}\right)^{\frac{f}{\gamma-1}}. \quad (5)$$

Figure 3 shows the profile for CH_4 ($f \sim 6$). We can see that the analytical solution matches the numerical model very well; in the lower atmosphere, where $D_0 \ll K_0$, it behaves as a constant mixing ratio profile; and in the upper atmosphere, where $D_0 \gg K_0$ and the pressure $p \propto e^{-\xi}$, it behaves as $\chi \propto p^f$.

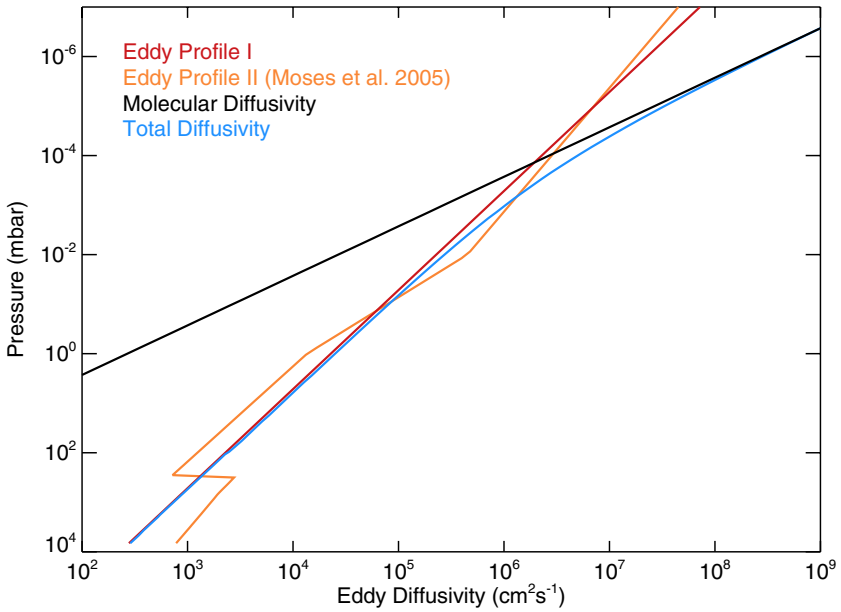

Figure 2. Profiles of eddy diffusivity and molecular diffusivity for CH_4 in the idealized model (eddy profile I) compared with the full chemistry models (eddy profile II). The blue curve is the total diffusivity for the idealized model.

(A color version of this figure is available in the online journal.)

Table 1
Analytical Solutions for the 1D Cases

	Case	Condition	Solution
Without wind $w_0 = 0$	I	$P_0 = L_0 = 0$, $D_0 \neq 0$	$\chi(\xi) = \frac{FH}{fN_0D_0} + \left(C_1 - \frac{FH}{fN_0D_0}\right)\left(\frac{D_0e^{(1-\gamma)\xi}+K_0}{D_0+K_0}\right)^{\frac{f}{\gamma-1}}$
	II	$P_0 = L_0 = D_0 = 0$	$\chi(\xi) = C_1 + \frac{e^{(1-\gamma)\xi}}{K_0(1-\gamma)}\frac{FH}{N_0}$
	III	$P_0 = D_0 = 0$	$\chi(\xi) = e^{\frac{(1-\gamma)\xi}{2}}\left[C_1I_\nu\left(\frac{2H\sqrt{\frac{L_0}{K_0}}}{\lvert\beta-\gamma\rvert}e^{\frac{(\beta-\gamma)\xi}{2}}\right) + C_2K_\nu\left(\frac{2H\sqrt{\frac{L_0}{K_0}}}{\lvert\beta-\gamma\rvert}e^{\frac{(\beta-\gamma)\xi}{2}}\right)\right]$, where $\nu = \left\lvert\frac{1-\gamma}{\beta-\gamma}\right\rvert$
	IV	$P_0 = K_0 = 0$	$\chi(\xi) = e^{\frac{-f\xi}{2}}\left[C_1I_\nu\left(\frac{2H\sqrt{\frac{L_0}{D_0}}}{\lvert\beta-1\rvert}e^{\frac{(\beta-1)\xi}{2}}\right) + C_2K_\nu\left(\frac{2H\sqrt{\frac{L_0}{D_0}}}{\lvert\beta-1\rvert}e^{\frac{(\beta-1)\xi}{2}}\right)\right]$, where $\nu = \left\lvert\frac{f}{\beta-1}\right\rvert$
	V	$L_0 = K_0 = 0$	$\chi(\xi) = \frac{P_0H^2}{D_0(f\alpha+\alpha^2)}e^{\alpha\xi} + C_1e^{-f\xi} + C_2$
	VI	$L_0 = D_0 = 0$	$\chi(\xi) = \frac{P_0H^2}{K_0\alpha(\alpha+1-\gamma)}e^{(\alpha+1-\gamma)\xi} + C_1e^{(1-\gamma)\xi} + C_2$
With wind $w_0 \neq 0$	VII	$P_0 = L_0 = D_0 = 0$	$\chi(\xi) = \frac{F}{w_0N_0}\left(e^{\frac{w_0H(e^{(1-\gamma)\xi}-1)}{K_0(1-\gamma)}} - C_2\right)$
	VIII	$K_0 = D_0 = 0$, $\alpha = \beta - 1$, $\beta \neq 0$	$\chi(\xi) = \frac{P_0}{L_0} + C_1e^{-\frac{L_0H}{w_0\beta}e^{\beta\xi}}$

Notes. See Section 3 in the text for details.

1. F represents a constant flux. See the text for definitions of other variables.
2. I_ν and K_ν are the modified Bessel functions of the first and second kinds, respectively. An asymptotic property of Bessel function is that, for small x, $I_\nu(x) \propto x^\nu$ and $K_\nu(x) \propto x^{-\nu}$. Therefore, in the limit of $L_0 \to 0$, the two solutions for cases II and III will be reduced to simple power-law profiles as functions of p, consistent with what we showed in the no-chemistry case (case I).
3. In the limit of $P_0 \to 0$, the two solutions for cases V and VI will approach the no-chemistry solutions: cases I and II, respectively.

3.1.2. C_2H_6

On the other hand, Jupiter's C_2H_6 is formed around the homopause region and transported downward. Therefore, the flux term cannot be ignored. Outside the source region, the photochemical loss of C_2H_6 can be neglected, and therefore the solution is like that for case I. Interestingly, the flux is also on the order of 10^9 cm^2 s^{-1} (Moses et al. 2005), implying a significant amount of carbon from methane ends up in ethane. FH/fN_0D_0 is $\sim 10^{-5}$ in the solution of case I. For C_2H_6, $f \sim 12$. Since the source of C_2H_6 is in the upper atmosphere, we can set the lower boundary condition as

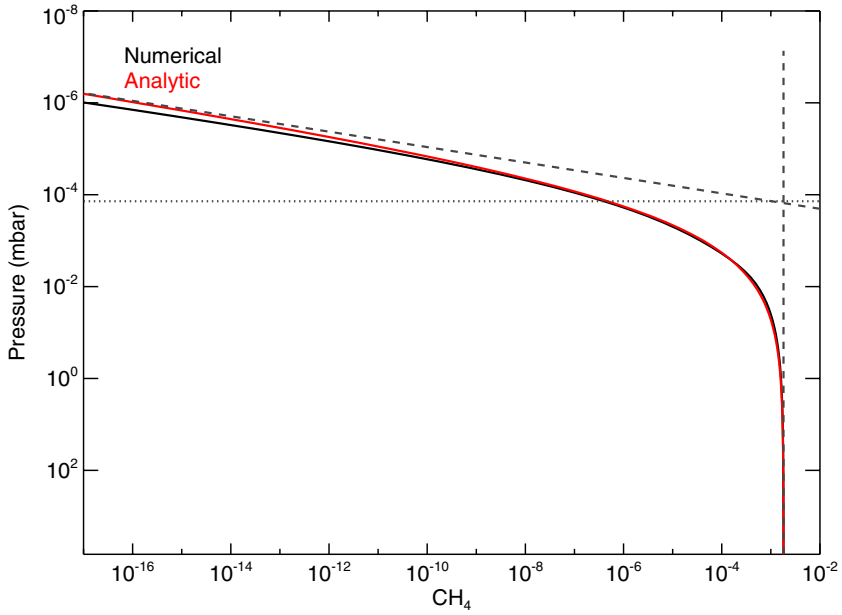

Figure 3. CH_4 from numerical simulations compared with analytical solutions. The dashed lines are asymptotic profiles. The dotted line indicates the homopause pressure level.

(A color version of this figure is available in the online journal.)

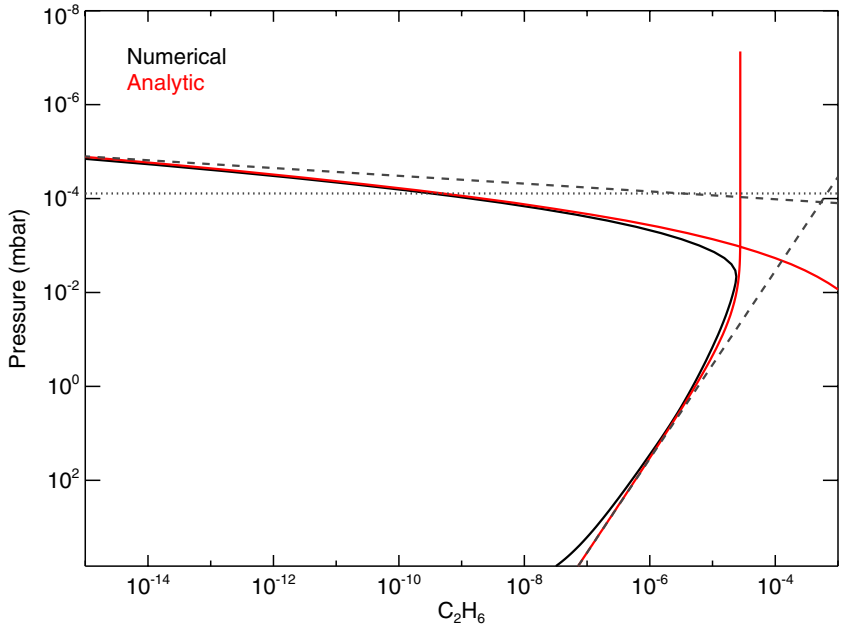

Figure 4. C_2H_6 from numerical simulations compared with analytical solutions. The dashed lines are asymptotic profiles. The dotted line indicates the homopause pressure level.

(A color version of this figure is available in the online journal.)

$\chi_0 = 0$, so the solution becomes

$$\chi(\xi) = \frac{FH}{f N_0 D_0}\left[1 - \left(\frac{D_0 e^{(1-\gamma)\xi} + K_0}{D_0 + K_0}\right)^{\frac{f}{\gamma-1}}\right]. \quad (6)$$

Figure 4 shows that the analytical solution matches the model result very well below the homopause. In the lower atmosphere, where $D_0 \ll K_0$, we take the Taylor expansion of the solution and obtain

$$\chi(\xi, D_0 \ll K_0) = \frac{FH(e^{(1-\gamma)\xi} - 1)}{K_0 N_0 (1-\gamma)}, \quad (7)$$

which is consistent with the solution for $D_0 = 0$ (case II). The solution implies that the C_2H_6 mixing ratio profile should asymptotically behave as $\chi \propto p^{(\gamma-1)}$ (Figure 4).

Above the source region the flux changes sign (upward), but since the flux drops fast, we can still ignore it, and the following

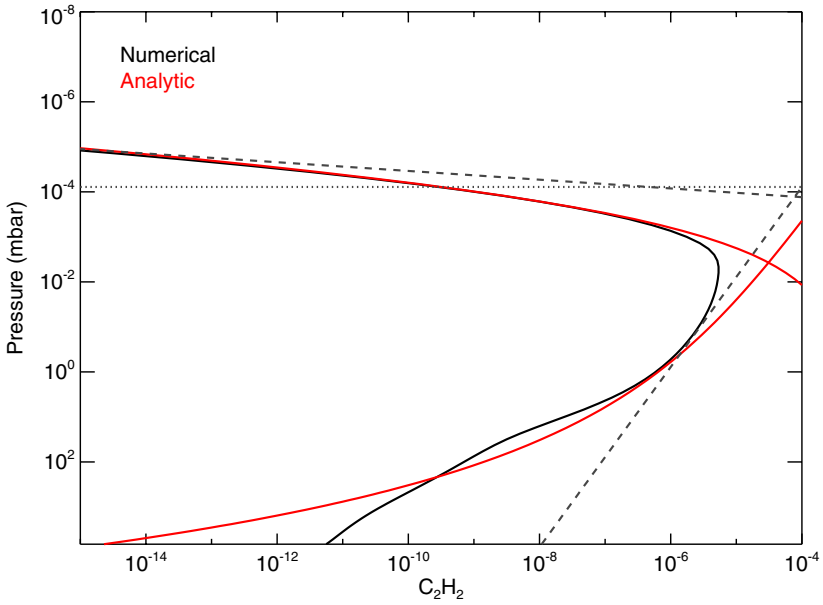

Figure 5. C_2H_2 from numerical simulations compared with analytical solutions. The dashed lines are asymptotic profiles. The dotted line indicates the homopause pressure level.

(A color version of this figure is available in the online journal.)

analytical solution matches the model result well, similar to the condition of CH_4. Let $F = 0$ in the solution of case I and note that at the homopause $D_0 e^{(1-\gamma)\xi} = K_0$,

$$\chi(\xi) = \chi_h \left[\frac{D_0 e^{(1-\gamma)\xi} + K_0}{2K_0} \right]^{\frac{f}{\gamma-1}}, \quad (8)$$

where χ_h is the volume mixing ratio at the homopause.

Because the analytical profiles are in agreement with a state-of-the-art Jupiter model from Moses et al. (2005), which is consistent with the current observations, we conclude that the Jovian stratospheric CH_4 and C_2H_6 are mostly in diffusive equilibrium, especially in the region where transport is much faster than the chemical processes.

3.1.3. C_2H_2

Above the homopause, the C_2H_2 profile can be approximated by the diffusive equilibrium (case I, with $F = 0$), as we showed for the C_2H_6 profile above the homopause. The analytical solution agrees very well with the numerical simulations (Figure 5). In the eddy-diffusion-dominated region, the solution of case III is a good approximation for the vertical profile of C_2H_2. C_2H_2 is transported downward, with additional sources from the photodissociation of C_2H_6 and C_2H_4. The C_2H_2 photolysis is a null chemical cycle because the products, C_2 and C_2H, will be quickly recycled back to C_2H_2 through reactions with H_2 and CH_4. The net chemical loss of C_2H_2 involves combining with a hydrogen atom to form C_2H_3, which is partly recycled back to C_2H_2. Given the sources and sinks, the net chemical loss timescale of C_2H_2 is $\sim 10^9$ s so that $L_0 \sim 10^{-9}\,s^{-1}$ in the solution of case III. For simplicity, we assume the loss timescale is approximately a constant with altitude, i.e., $\beta \sim 0$. $\chi(\xi)$ is expected to increase with altitude for the source region above and we assume the lower boundary is $\chi(0) = 0$. Therefore, the I_ν term is ignored ($C_1 = 0$). In the solution of case III, $\nu = |(1-\gamma)/(\beta-\gamma)| = 1$ and $2H\sqrt{L_0/K_0} \sim 9$. The analytical C_2H_2 profile, as shown in Figure 5, is

$$\chi(\xi) = 5 \times 10^{-7} e^{\frac{\xi}{4}} K_1\left(18 e^{\frac{\xi}{4}}\right). \quad (9)$$

Here $C_2 = 5 \times 10^{-7}$ is based on the source flux from the region above. The profile qualitatively agrees with the model result, although not as well as the CH_4 and C_2H_6 cases in Section 3.1.1 because we simplified the chemistry. But we conclude that the C_2H_2 profile on Jupiter can be approximated by the modified Bessel function K_ν.

Unlike Jovian C_2 hydrocarbons that are primarily in diffusive equilibrium above the homopause, some strong UV absorbers, such as carbon dioxide in upper atmospheres of Earth and maybe other exoplanets, would fall off very rapidly owing to both molecular diffusion and photolysis. The solution in case IV provides a good estimate of the vertical profiles of those species.

If the chemical production rate is much larger than the chemical loss rate in the region we are interested in, the species will either diffuse downward with a loss due to the thermodecomposition or dry deposition in the lower atmosphere, such as some higher order hydrocarbons or aerosol precursors, or diffuse upward and escape from the upper atmosphere, such as the atomic hydrogen in upper atmospheres of hot Jupiters. In those cases, we can solve the chemical-diffusive system by neglecting the chemical loss term. However, the analytical solutions generally contain the hypergeometric functions. In two simple cases, cases V and VI, we provide the analytical solutions for the regions above and below the homopause, respectively.

3.2. Cases with Wind

If we define a new "mass factor" $f^* = f - (w_0 H/D_0)$, Equation (4) will be reduced to the wind-free case that we discussed in Section 3.1. The physical meaning of the correction factor $w_0 H/D_0$ is the ratio of the molecular diffusive timescale to the vertical advection timescale. Naively we can imagine an upward wind tends to make the gas molecule "lighter," while a downward wind will make the species "heavier." This result can be directly applied to CH_4, as shown in Figure 6, with $w_0 = \pm 5 \times 10^{-8}\,cm\,s^{-1}$. Due to the difficulty of measuring the vertical wind velocity in the real planetary atmospheres, the w_0 values are chosen according to the loss timescale and vertical diffusion timescale of CH_4 so as to show the influences of the

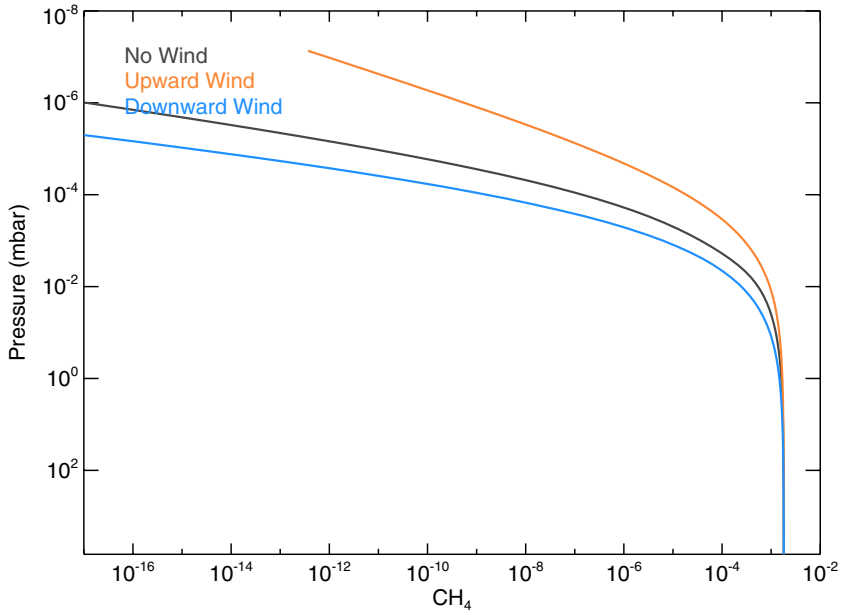

Figure 6. Analytical CH_4 profiles from the cases with and without wind. $w_0 = \pm 5 \times 10^{-8}$ cm s^{-1}.
(A color version of this figure is available in the online journal.)

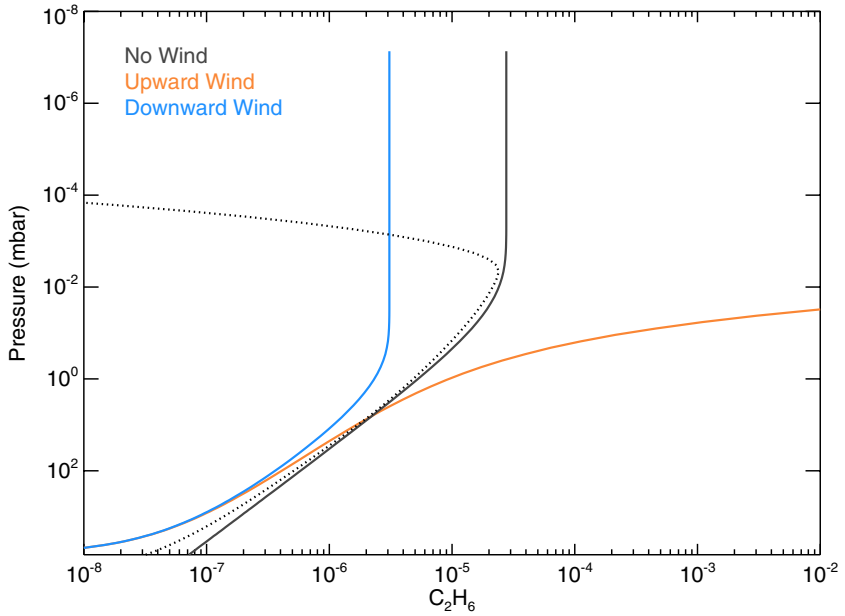

Figure 7. Analytical C_2H_6 profiles from the cases with and without wind. $w_0 = \pm 1 \times 10^{-6}$ cm s^{-1}. The dotted line shows a solution with the molecular diffusion in the upper atmosphere.
(A color version of this figure is available in the online journal.)

wind. It is not proper to put the wind into numerical simulations, as it will cause numerical problems. We show the analytical solutions only for qualitative illustration. The results show that an upward wind will lift up the homopause and a downward wind will push it down. It actually transports the more (less) abundant species from below (above) and thus increases (decreases) the mixing ratio of CH_4.

In the 2D simulation, we generally care most about the region below the homopause, because most of the latitudinal observations of Jupiter come from around 1 mbar, or some lower altitude. Therefore, we examine solutions in which the only diffusivity is eddy diffusivity. If we neglect the chemical production and loss terms, the solution (case VII) would have a different slope from the solutions in the wind-free cases. The solution depends on the ratio of the diffusion timescale to the advection timescale, $w_0 H/K_0$. Figure 7 shows two typical vertical profiles of C_2H_6, with an upward wind and downward wind ($\sim w_0 = \pm 1 \times 10^{-6}$ cm s^{-1}), compared with the wind-free theoretical curve. It shows that an upward wind will increase the mixing ratio in the higher altitude by preventing the species from being transported downward, but a downward wind tends to lower the mixing ratio of C_2H_6. Therefore, if we neglect the horizontal transport, the rising air at the equator and sinking air at the poles will result in more C_2H_6 at the equator and less C_2H_6 at the poles, which is contradicted by the CIRS measurements (Zhang et al. 2013). That suggests the horizontal transport is

Table 2
Analytical Solutions for the Pure Advective 2D Cases

Case	IX	X
Stream function	ψ_A: $\psi(\theta,\xi) = a w_0 e^{\eta\xi} \sin\theta \cos^2\theta$	ψ_B: $\psi(\theta,\xi) = a w_0 e^{\eta\xi} \cos^2\theta$
Production	$P(\theta,\xi) = P_0 N_0 (\cos\theta)^{\frac{-L_0 H}{(\eta-1)w_0}}$	$P(\theta,\xi) = P_0 N_0 \left(\frac{1+\sin\theta}{1-\sin\theta}\right)^{\frac{L_0 H}{2(\eta-1)w_0}}$
Loss	$L(\theta,\xi) = L_0 N_0 e^{(\eta-1)\xi} \sin^2\theta\chi$	$L(\theta,\xi) = L_0 N_0 e^{(\eta-1)\xi}\chi$
Solution	$\chi(\theta,\xi) = (\cos\theta)^{\frac{-L_0 H}{(\eta-1)w_0}} \left[G(e^{-\xi}\psi) - \frac{P_0 a H \sin\theta}{(\eta-1)e^{-\xi}\psi}\right]$	$\chi(\theta,\xi) = \left(\frac{1+\sin\theta}{1-\sin\theta}\right)^{\frac{L_0 H}{2(\eta-1)w_0}} \left[G(e^{-\xi}\psi) - \frac{P_0 a H \sin\theta}{(\eta-1)e^{-\xi}\psi}\right]$

actually important and this "pseudo-2D" photochemical model is not sufficient to explain the observations. In some planetary atmospheres, such as regions with strong upward or downward winds (e.g., dayside or nightside of hot Jupiters), transport by eddy diffusion may be neglected compared with vertical wind advection. However, when we add the chemical source/loss, the equation cannot be solved analytically in general. Case VIII provides a special solution if the chemical production and loss terms are specified and satisfy $\alpha = \beta - 1$ and $\beta \neq 0$.

4. 2D SYSTEM IN THE MERIDIONAL PLANE

Consider a 2D chemical–advective–diffusive system below the homopause in the latitudinal and vertical coordinate. We still assume the atmosphere to be isothermal and barotropic. From previous experience, we note that the equation with eddy diffusion ($\gamma \sim 0.5$), advection and chemistry all together cannot be solved analytically, even in the 1D case. Therefore, we are trying to decouple the processes. We introduce the stream function ψ so that

$$v = -\frac{1}{\cos\theta} e^{\xi} \frac{\partial}{\partial z}(e^{-\xi}\psi), \tag{10a}$$

$$w = \frac{1}{\cos\theta}\frac{\partial\psi}{\partial y}. \tag{10b}$$

4.1. Without Chemistry, $P_0 = L_0 = 0$

If the chemistry can be ignored, the steady state of Equation (1) becomes

$$v\frac{\partial\chi}{\partial y} + w\frac{\partial\chi}{\partial z} - \frac{1}{\cos\theta}\frac{\partial}{\partial y}\left(\cos\theta\ K_{yy}\frac{\partial\chi}{\partial y}\right) - e^{\xi}\frac{\partial}{\partial z}\left(e^{-\xi}K_{zz}\frac{\partial\chi}{\partial z}\right) = 0. \tag{11}$$

If we also neglect the eddy diffusion term, the solution would be trivial: for any given stream function ψ, the solution is $\chi(\theta,\xi) = G(e^{-\xi}\psi(\theta,\xi))$, where G is any functional form determined by the boundary conditions and $e^{-\xi}\psi$ is the mass-weighted stream function. On the other hand, by ignoring the advection term, we have a 2D diffusion equation. But this solution will be trivial too because there is no horizontal diffusion flux without a chemical source. It will be reduced to the 1D case.

4.2. With Chemistry

Let us introduce the chemistry. The source and sink terms are parameterized as $P(\theta,\xi) = P_0 N_0 e^{\alpha\xi} f(\theta)$ and $L(\theta,\xi) = L_0 N e^{\beta\xi} g(\theta)\chi = L_0 N_0 e^{(\beta-1)\xi} g(\theta)\chi$.

4.2.1. Pure Advection Cases

The general approach to solving the pure advection 2D cases is discussed in Appendix A. We introduced two typical circulation patterns: (1) an axis-symmetric equator-to-pole circulation pattern in each hemisphere, called ψ_A, and (2) a global pole-to-pole circulation pattern, called ψ_B. The solutions are summarized in Table 2.

We now test our numerical model against analytical solutions. The numerical model has dimensions 80 × 33, with 80 pressure grid points from 100 mbar to 5 mbar, and 33 latitudes from 85°S to 85°N with increments of 5°. Two numerical schemes are tested. In the first scheme, called the "normal 2D" mode, the photochemistry, diffusion, and advection are solved together using a time-marching method (Shia et al. 1990). In the second scheme, called the "quasi 2D" mode (Liang et al. 2005), first we perform a series of 1D calculations at different latitudes using the matrix inversion method (see Section 3), and then the meridional advection and horizontal diffusion are applied to connect different latitudes. Our calculations show that when reaching the steady state, the two modes converge in the same solution. But the "quasi 2D" mode takes a shorter time to reach the steady state than the "normal 2D" mode, because the former allows large time steps in the 1D diffusion calculation but the latter is limited by the CFL criterion for every time step.

We assume the Jupiter value $N_0 = 4.83 \times 10^{18}\,\mathrm{g\,cm^{-3}}$ at 100 mbar and planetary radius $a = 7.1824 \times 10^9$ cm. We assume $P_0 = 10^{-16}\,\mathrm{cm^{-3}\,s^{-1}}$, $w_0 = 10^{-3}\,\mathrm{cm\,s^{-1}}$, $H = 2.5 \times 10^5$ cm, and $\eta = 0.3$. So the transport timescale is about 3×10^9 s. For each circulation pattern, we tested two fictitious chemical tracers, a short-lived tracer with loss rate faster than transport ($L_0^{-1} = 10^9$ s) and a long-lived tracer with loss rate slower than transport ($L_0^{-1} = 10^{11}$ s).

In the case of Jupiter with nearly no obliquity, we hypothesize the circulation pattern to be axis-symmetric (ψ_A), in which air rises at the equator and sinks at the poles. Our analytical solution is given in case IX, with $G(e^{-\xi}\psi) = 5 \times 10^{-19}(e^{-\xi}\psi)^2$. For the other circulation pattern, which might be relevant to the planets with large obliquity, such as Earth or Titan, air rises at the south pole and sinks at the north pole, and our analytical solution is given in case X, with $G(e^{-\xi}\psi) = -0.26(e^{-\xi}\psi)^{-1}$. We use the boundary values from the analytical solutions for the numerical model. The mass stream functions are shown in Figures 8 and 9, respectively. The production term in case IX represents a common cosine-shaped photochemical production function modulated by the solar flux; while that in case X with a trend from one pole to the other is actually simulating a possible polar source, e.g., from ion-chemistry in the aurora region. The loss term in case IX can be considered as an ion-chemical loss which peaks at the poles, while that in case X is a common linear loss approximation for a certain loss timescale.

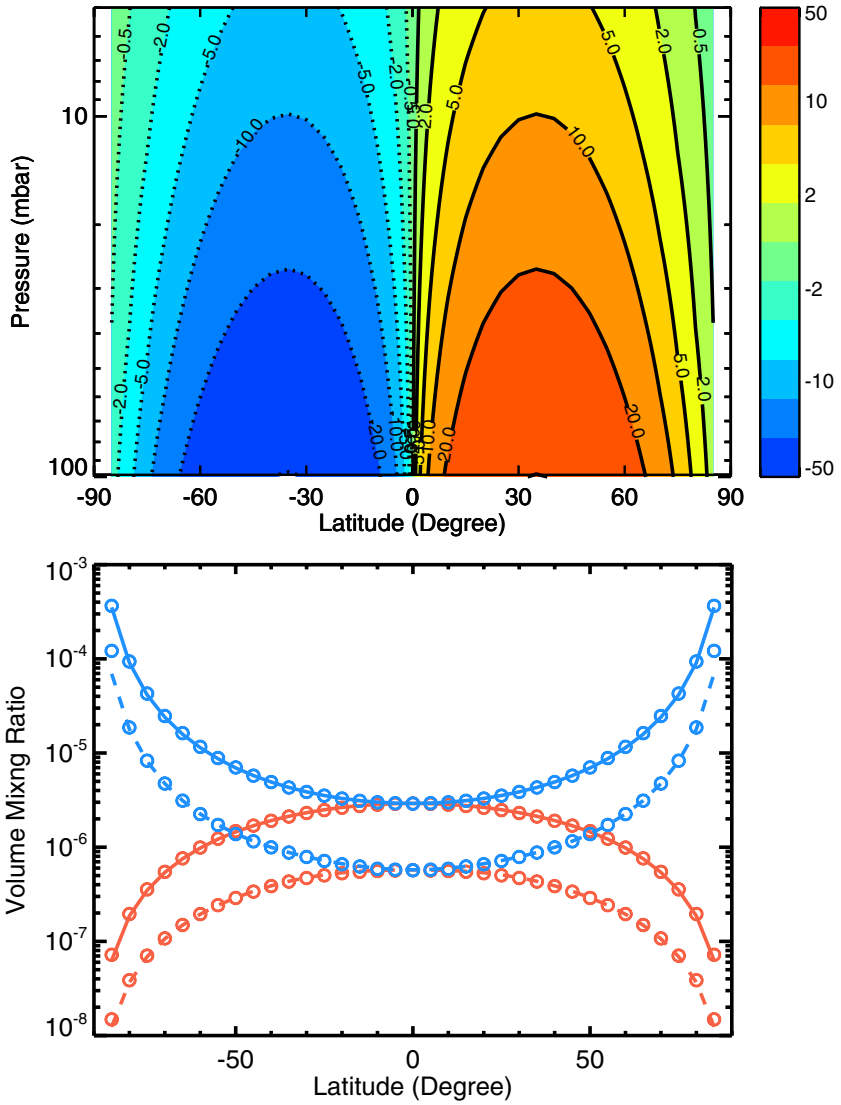

Figure 8. Plots of case IX. Upper panel: analytic mass stream functions in units of g cm^{-1} s^{-1}. Bottom panel: comparison of analytical (lines) and numerical (dots) solutions for two fictitious chemical tracers, the short-lived tracer (orange) and the long-lived tracer (blue). The solid and dashed curves correspond to 5 and 50 mbar, respectively.

(A color version of this figure is available in the online journal.)

The results from case IX are plotted in Figure 8, with the numerical simulation results (dots) on top of each curve. For the short-lived tracer, chemical production and loss dominate its local abundances. Because the production is higher at the equator and loss is higher at the poles, the steady-state mixing ratio of the short-lived tracer is higher in the low latitudes and lower in the high latitudes. On the other hand, the latitudinal distribution of the long-lived species is dominated by the transport. It exhibits an opposite latitudinal trend to that of the short-lived species, with higher mixing ratio in the higher latitudes and lower mixing ratio in the lower latitudes. The numerical results are based on our 2D CTM (Caltech/JPL kinetics model), which is able to reproduce the analytical results almost perfectly. The largest differences between the analytical and numerical simulations are found at the two poles, but are still less than 4%. Case IX qualitatively interprets the opposite latitudinal distributions between C_2H_2 (a short-lived species) and C_2H_6 (a long-lived species), as revealed by the *Cassini* and *Voyager* observations (Zhang et al. 2013).

Similar behavior appears in the results from case X (Figure 9). Although both tracers have higher production rates in the southern hemisphere and linear loss rate coefficients independent of latitude, their steady-state latitudinal distributions are significantly different. Again, the short-lived tracer is dominated by the chemistry, while the long-lived tracer shows transport-dominant behavior.

4.2.2. Pure Diffusive Cases

Ignoring the advection terms, we now have a 2D diffusion equation

$$\frac{1}{a^2\cos\theta}\frac{\partial}{\partial\theta}\left(\cos\theta K_{yy}\frac{\partial\chi}{\partial\theta}\right)+\frac{e^{\xi}}{H^2}\frac{\partial}{\partial\xi}\left(K_0e^{(\gamma-1)\xi}\frac{\partial\chi}{\partial\xi}\right)+P_0e^{(\alpha+1)\xi}f(\theta)-L_0e^{\beta\xi}g(\theta)\chi=0. \quad (12)$$

Generally there is no analytical solution for this equation. If we further assume the solution of the 2D diffusion equation can be expressed as $\chi(\theta,\xi)=A(\theta)G(\xi)$, and let $G(\xi)=C_1e^{(1-\gamma)\xi}$,

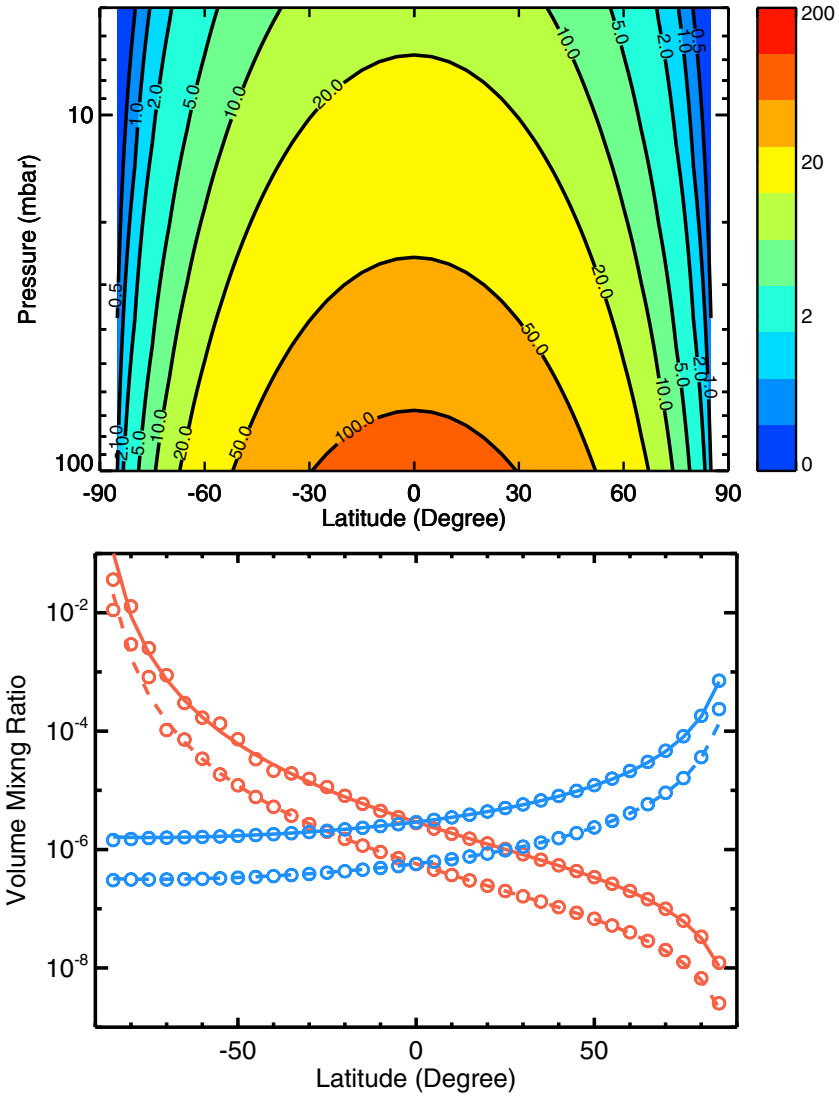

Figure 9. Plots of case X. Upper panel: analytic mass stream functions in units of $\mathrm{g\,cm^{-1}\,s^{-1}}$. Bottom panel: comparison of analytical (lines) and numerical (dots) solutions for two fictitious chemical tracers, the short-lived tracer (orange) and the long-lived tracer (blue). The solid and dashed curves correspond to 5 and 50 mbar, respectively.

(A color version of this figure is available in the online journal.)

Table 3
Analytical Solutions for the Pure Diffusive 2D Cases

Case	Production	Loss	Solution
XI	$P(\theta,\xi) = P_0 N_0 e^{-\gamma\xi}$	$L(\theta,\xi) = L_0 N_0 e^{-\xi}\chi$	$\chi(\theta,\xi) = C_1 e^{(1-\gamma)\xi}\left[P_\nu(\sin\theta) - \frac{2}{\pi}\tan\left(\frac{\pi\nu}{2}\right)Q_\nu(\sin\theta) + \frac{P_0}{C_1 L_0}\right]$
XII	$P(\theta,\xi) = P_0 N_0 e^{-\gamma\xi}$	$L(\theta,\xi) = 0$	$\chi(\theta,\xi) = \left[C_1 + \frac{a^2 P_0}{2K_{yy}}\ln(\cos^2\theta)\right]e^{(1-\gamma)\xi}$
XIII	$P(\theta,\xi) = P_0 N_0 e^{-\gamma\xi}\cos^2\theta$	$L(\theta,\xi) = 0$	$\chi(\theta,\xi) = \left\{C_1 + \frac{a^2 P_0}{6K_{yy}}[-\sin^2\theta + 2\ln(\cos^2\theta)]\right\}e^{(1-\gamma)\xi}$
XIV	$P(\theta,\xi) = P_0 N_0 e^{-\gamma\xi}\sin^2\theta$	$L(\theta,\xi) = 0$	$\chi(\theta,\xi) = \left\{C_1 + \frac{a^2 P_0}{6K_{yy}}[\sin^2\theta + \ln(\cos^2\theta)]\right\}e^{(1-\gamma)\xi}$

Note. P_ν and Q_ν are the Legendre functions of the first and second kinds, respectively.

$\alpha = -\gamma$, and $\beta = 0$, the solutions for the pure diffusion 2D cases are discussed in Appendix B. Four typical cases are summarized in Table 3. In the numerical simulations, we assume $P_0 = 10^{-16}\,\mathrm{cm^{-3}\,s^{-1}}$, $L_0^{-1} = 10^{11}\,\mathrm{s}$, and $\gamma = 0.1$. The results are plotted in Figure 10.

In case XI, we assume the production rate is uniform at the top and the loss rate linear. $C_1 = 0$ in the solution leads to a trivial case with a constant mixing ratio with latitude. If $C_1 \neq 0$, the solution will exhibit a horizontal diffusional equilibrium. We assume $K_{yy} = 2.1 \times 10^9\,\mathrm{cm^2\,s^{-1}}$ in the numerical simulations, consistent with the order of magnitude from the previous numerical estimations (e.g., Friedson et al. 1999; Liang et al. 2005). The solution shows a bowl-shaped distribution with a minimum value at the equator and maximum value at the poles (Figure 10). So the horizontal flux is from pole to equator. At any latitude there should be a flux convergence to balance the

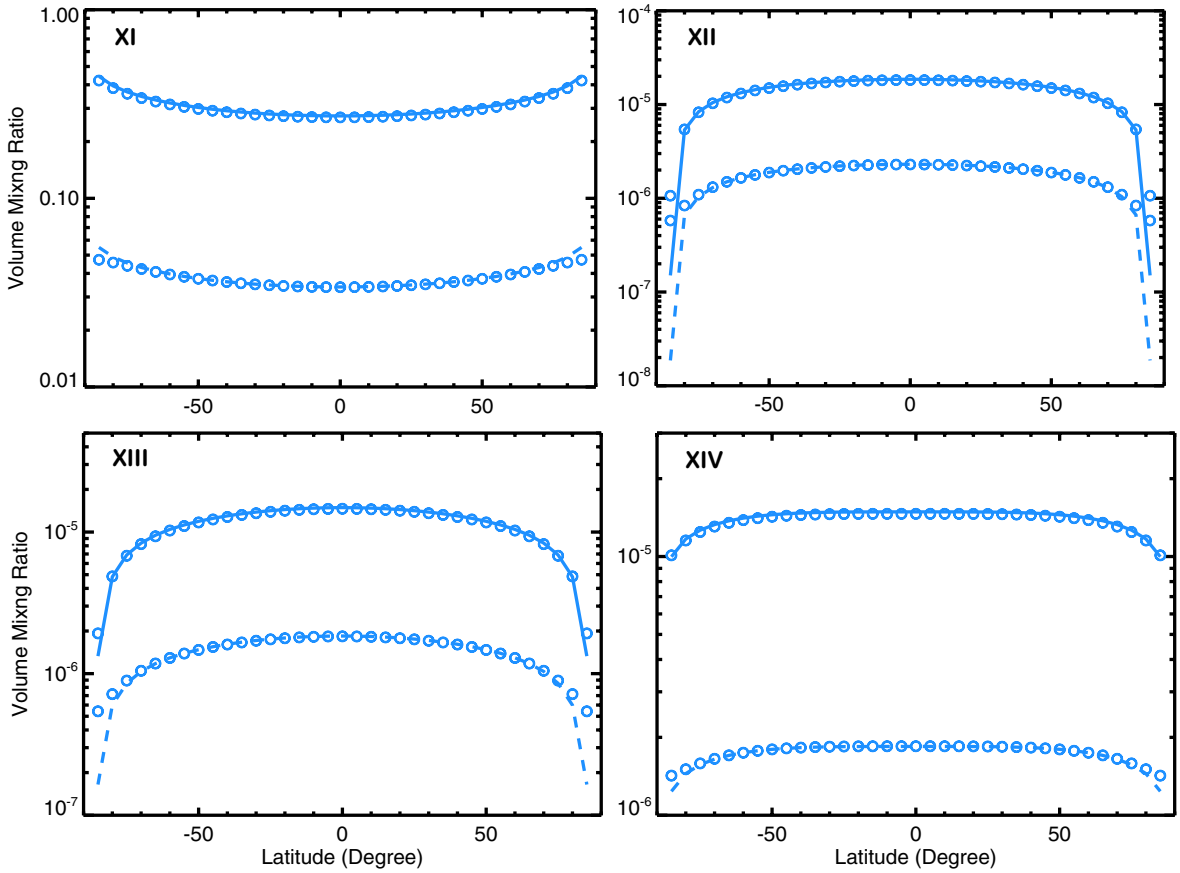

Figure 10. Comparison of analytical (lines) and numerical (dots) solutions for the pure diffusive 2D cases XI, XII, XIII, and XIV in Table 3. The case number is indicated in each panel. The solid and dashed curves correspond to 5 and 50 mbar, respectively.

(A color version of this figure is available in the online journal.)

chemical loss. The area-weighted loss rate has a maximum at equator, therefore a maximum flux convergence as well.

If the production rate is non-uniform at the top and there is no chemical loss, the analytical solutions for case XII ($n = 0$) and case XIII ($n = 1$) exist. In the numerical simulations, we assume $K_{yy} = 1 \times 10^9$ cm^2 s^{-1}. The solutions show an upside-down bowl-shaped distribution with the maximum value at the equator and a sharp falloff in the polar region (Figure 10). So the horizontal flux is from equator to pole. Since there is no chemical loss in these cases, at any latitude there should be a flux divergence to balance the chemical production. The solutions demonstrate that if the chemical loss can be ignored, any diffusive transport process with a chemical production rate that is either flat ($n = 0$ in Appendix B) or peaked ($n = 1$) in the low latitudes will result in a high mixing ratio in the low latitudes. Therefore, the horizontal mixing solution of C_2H_6, whose chemical loss can be ignored, will have an upside-down bowl shape. Our simple analytical cases are consistent with the model results in Liang et al. (2005) and Lellouch et al. (2006), but not with the *Voyager* and *Cassini* data (Zhang et al. 2013). We note that the ratio of the production rate with the horizontal mixing determines the "flatness" of the bowl-shape distribution. A more efficient horizontal mixing leads to a flatter distribution. The horizontal timescale should be much shorter than the chemical production timescale in the Liang et al. (2005) case, which is correct because in the lower atmosphere chemical production of C_2H_6 is not efficient. The observed latitudinal distribution from CIRS implies either that the mean residual circulation plays an important role or that there is a chemical source of C_2H_6 in the polar region. So far, there is no evidence of any ion chemistry initiated by precipitating particles in the aurora region that would enhance the ethane abundances. Any chemical mechanism proposed to enhance C_2H_6 near the poles must not tend to increase C_2H_2, as the observations show that C_2H_2 is not enhanced at the poles, even though in principle C_2H_2 should be more sensitive to local chemical sources because of its shorter lifetime.

The solution (case XIV) also shows a bowl-shaped distribution with the maximum value at the equator and minimum value at the poles (Figure 10). So if we ignore the advection terms, the required latitudinal slope of the production rate of C_2H_6 should be much steeper than the $\sin^2\theta$ in order to explain the CIRS observations. Numerical simulations with more realistic chemistry and eddy mixing are needed to confirm this hypothesis.

5. 2D SYSTEM IN THE ZONAL PLANE

If we consider the system in an altitude–longitude plane, which is appropriate for slowly rotating planets such as Venus and hot Jupiters, a strong subsolar–anti-solar circulation coupled with the zonal jets, and with the inhomogeneous production rate, will lead to a different scenario. In the zonal plane, the horizontal eddy diffusion can be neglected. In the steady state, the governing equation is

$$\frac{u}{a}\frac{\partial \chi}{\partial \lambda} + w\frac{\partial \chi}{\partial z} - e^{\xi}\frac{\partial}{\partial z}\left(e^{-\xi}K_{zz}\frac{\partial \chi}{\partial z}\right) = \frac{P-L}{N}. \quad (13)$$

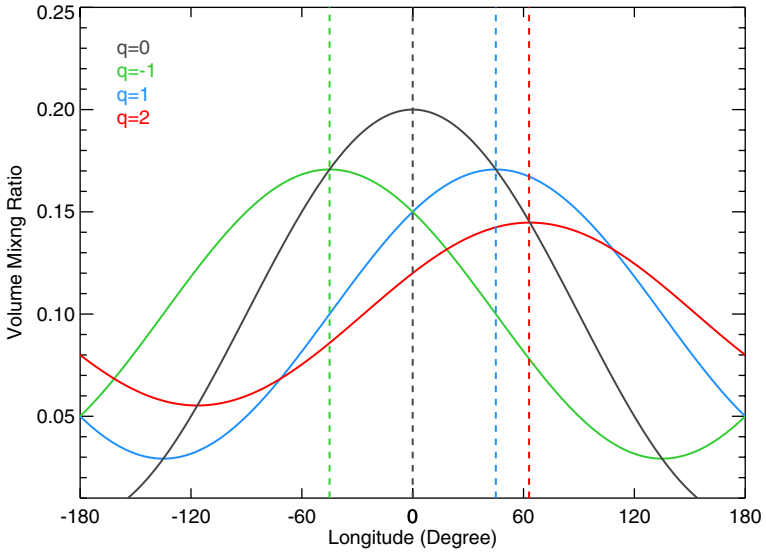

Figure 11. Analytical solutions at $\xi = 0$ for the zonal transport cases. Different ratios (q values) of the transport vs. chemical timescales result in different phase lags and different amplitudes of the longitudinal mixing ratio profiles. The dashed lines indicate the longitudes corresponding to the peaks of the mixing ratio profiles. The chemical source distribution follows a cosine function with its peak at longitude 0°.

(A color version of this figure is available in the online journal.)

where λ is the longitude, and a is the radius of the latitude circle. We can formulate the stream function ψ in the zonal and vertical plane:

$$u = -e^{\xi}\frac{\partial}{\partial z}(e^{-\xi}\psi), \tag{14a}$$

$$w = \frac{1}{a}\frac{\partial \psi}{\partial \lambda}. \tag{14b}$$

If we neglect the diffusion term, this is basically the same as the 2D problem in the meridional plane, but without the $\cos\theta$ factor. The solution is related to the subsolar–anti-solar circulation, which is analogous to the equator-pole circulation problem (case IX).

We can also simply solve the problem by neglecting the vertical advection term in Equation (13). Suppose a fast jet rapidly flows along the latitude circle with a constant velocity u, and that the air mass is approximately conserved in that altitude over a short timescale, as with the four-day zonal wind on Venus and fast zonal jets on hot Jupiters. The vertical profile is modified by the eddy diffusion. As usual, we assume $P(\lambda, \xi) = P_0 N_0 e^{\alpha\xi} f(\lambda)$, $L(\lambda, \xi) = L_0 N_0 e^{(\beta-1)\xi} g(\lambda)\chi$, and $K_{zz} = K_0 e^{\gamma\xi}$. Equation (13) becomes

$$\frac{u}{a}\frac{\partial \chi}{\partial \lambda} - e^{\xi}\frac{\partial}{\partial z}\left(K_0 e^{(\gamma-1)\xi}\frac{\partial \chi}{\partial z}\right) - P_0 e^{(\alpha+1)\xi} f(\lambda) + L_0 e^{\beta\xi} g(\lambda)\chi = 0. \tag{15}$$

Let us check a simple case with a special solution. Similar to the argument of the 2D diffusive system, we let $\alpha = -\gamma$ and $\beta = 0$, and we assume the solution can be expressed as $\chi(\lambda, \xi) = A(\lambda)G(\xi)$, where $G(\xi) = C_1 e^{(1-\gamma)\xi}$. The solution is

$$\chi(\lambda, \xi) = e^{-\frac{aL_0}{u}\int g(\lambda)\,d\lambda}\left[C_1 + \frac{aP_0}{u}\int f(\lambda) e^{\frac{aL_0}{u}\int g(\lambda)\,d\lambda} d\lambda\right] e^{(1-\gamma)\xi}. \tag{16}$$

The periodic boundary condition, i.e., $\chi(0, \xi) = \chi(2\pi, \xi)$, requires C_1 to be 0. A simple case would be $f(\lambda) = 1 + \cos k\lambda$ and $g(\lambda) = 1$, where $k = 1$ stands for the two-modal production rate (day–night contrast). The solution would be

$$\chi(\lambda, \xi) = \frac{P_0}{L_0}\left[1 + \frac{1}{\sqrt{1+q^2}}\cos(k\lambda - \phi)\right] e^{(1-\gamma)\xi}, \tag{17}$$

where the dimensionless variable $q = ku/aL_0$ measures chemical loss timescale versus advection timescale (across an envelope of the production rate distribution). $\phi = \tan^{-1} q$ can be regarded as the phase lag of the mixing ratio distribution compared with the production rate distribution, and the amplitude of the mixing ratio variation is smaller than the production rate variation by a factor of $\sqrt{1+q^2}$. When the advection timescale and the chemical loss timescale are comparable, i.e., $q = 1$, the phase shift is 45°. If q is large, i.e., when the chemical loss is slower than the advection timescale, the zonal wind will quickly redistribute the chemicals and lead to a large phase lag and smooth the mixing ratio profile in longitude. On the other hand, if q is small, chemistry will dominate the distribution. Therefore, the phase lag due to advection would be smaller since the local chemical equilibrium will be established more quickly, leading to a large mixing ratio bulge along the latitude circle. Figure 11 illustrates some typical results at $\xi = 0$ for a range of values of q.

6. CONCLUDING REMARKS

In this study, we systematically investigated possible analytical benchmark cases in the chemical–advective–diffusive system. Although our solutions are highly idealized, we can still gain physical insights into what controls the vertical and latitudinal profiles of the short-lived and long-lived species in the stratosphere of Jupiter. In the 1D system, we show that CH_4 and C_2H_6 are mainly in diffusive equilibrium, and the C_2H_2 profile can be approximated by modified Bessel functions. Those analytical solutions could be used for the simple treatment of photochemistry in climate models or general circulation models. In the 2D system in the meridional plane, analytical solutions for two typical circulation patterns are derived. Simple tracer transport cases demonstrate that the distribution of short-lived

species is dominated by the local chemical sources and sinks, while that of the long-lived species is significantly influenced by the circulation. This may help solve the difference in the latitudinal distribution between C_2H_2 and C_2H_6, as revealed by the *Cassini* and *Voyager* spectra. On the other hand, it seems difficult for a pure diffusive transport process to produce the observed profile of C_2H_6, whose chemical loss can be neglected. Intuitively it also makes sense because the horizontal eddy mixing is not able to reverse the latitudinal gradient driven by the photochemistry. Unless there is a missing chemical source for C_2H_6 (but not for C_2H_2) in the polar region, the most probable solution is a meridional circulation from equator to pole. The detailed structure of the residual circulation in the stratosphere of Jupiter requires a realistic numerical simulation. For the slowly rotating planet, which might have longitudinally heterogeneous chemical sources, the interaction between the advection by the zonal wind and chemistry might cause a phase lag between the final tracer distribution and the original source distribution. The magnitude of the phase lag and longitudinal contrast of the tracer profile depend on the ratio of the advection timescale to the lifetime of the tracer. This is similar to the mechanism that causes a phase shift between the location of the atmospheric temperature maximum and sub-solar point (where heating is a maximum) on close-in giant planets (Knutson et al. 2007).

The analytical solutions have been used to validate the numerical simulations from our 2D Caltech/JPL CTM and show good agreement for various cases. The largest discrepancy usually appears in the polar region, especially when the analytical solutions have singular values at the poles, such as case XI. Increasing the horizontal and vertical resolution would lead to better agreement. This study lays the theoretical basis and provides numerical tools for future realistic chemistry-transport modeling in planetary and exoplanetary atmospheres.

We thank P. Gao, M. Line, M. Wong, Q. Zhang and other members of Yung's group for useful comments, and M. Gerstell for critical reading of the manuscript. This research was supported in part by NASA NNX09AB72G grant to the California Institute of Technology.

APPENDIX A

SOLUTIONS OF THE PURE ADVECTION 2D CASES

Consider a case without the eddy diffusion terms in Equation (1). In steady state,

$$v\frac{\partial \chi}{\partial y} + w\frac{\partial \chi}{\partial z} - p + l\chi = 0, \tag{A1}$$

where $p = P(\theta, \xi)/N$, and $l\chi = L(\theta, \xi)/N$.

With a stream function ψ introduced in Equation (10), Equation (A1) becomes

$$\frac{e^{\xi}}{aH\cos\theta}\left(\frac{\partial(e^{-\xi}\psi)}{\partial\theta}\frac{\partial\chi(\theta,\xi,G)}{\partial\xi} - \frac{\partial(e^{-\xi}\psi)}{\partial\xi}\frac{\partial\chi(\theta,\xi,G)}{\partial\theta}\right) - p + l\chi(\theta,\xi,G) = 0. \tag{A2}$$

Note that for any functional form G, the following relationship holds:

$$\frac{\partial(e^{-\xi}\psi)}{\partial\theta}\frac{\partial G(e^{-\xi}\psi)}{\partial\xi} - \frac{\partial(e^{-\xi}\psi)}{\partial\xi}\frac{\partial G(e^{-\xi}\psi)}{\partial\theta} = 0. \tag{A3}$$

Therefore, given $p(\theta,\xi) = P_0 e^{(\alpha+1)\xi} f(\theta)$, $l(\theta,\xi) = L_0 e^{\beta\xi} g(\theta)$, and $\psi(\theta,\xi) = \psi_1(\theta)\psi_2(\xi)$, we wish to find a solution using separation of variables in the form of $\chi(\theta,\xi,G) = A_1(\theta)A_2(\xi) + K_1(\theta)K_2(\xi)G(e^{-\xi}\psi)$. Substituting into Equation (A2), we obtain the following two ordinary differential equations:

$$\frac{d\ln(\psi_1)}{d\theta}\frac{d\ln(K_2)}{d\xi} - \frac{d\ln(e^{-\xi}\psi_2)}{d\xi}\frac{d\ln(K_1)}{d\theta} + \frac{L_0 aHg(\theta)\cos\theta e^{\beta\xi}}{\psi_1\psi_2} = 0, \tag{A4}$$

and

$$\frac{d\ln(\psi_1)}{d\theta}\frac{d\ln(A_2)}{d\xi} - \frac{d\ln(e^{-\xi}\psi_2)}{d\xi}\frac{d\ln(A_1)}{d\theta} + \frac{L_0 aHg(\theta)\cos\theta e^{\beta\xi}}{\psi_1\psi_2} - \frac{P_0 aHf(\theta)\cos\theta e^{(\alpha+1)\xi}}{A_1\psi_1 A_2\psi_2} = 0. \tag{A5}$$

The first equation is a special case of the second one. To get the analytical solution, we have to choose $f(\theta)$ and $g(\theta)$ carefully. We discuss the following two conditions:

1. Let $(d\ln(\psi_1)/d\theta) = r(d\ln(A_1)/d\theta)$; in order to solve for A_2, we need to diminish the θ terms in the production and loss terms, i.e., both $g(\theta)\cos\theta/(d\psi_1/d\theta)$ and $f(\theta)\cos\theta/(A_1 d\psi_1/d\theta)$ should be constants. Note that $w(\theta,\xi) = (1/\cos\theta)(\partial\psi/\partial y)$, therefore $g(\theta)/w(\theta,\xi)$ is a constant in latitude. However, the vertical velocity $w(\theta,\xi)$ could be positive or negative for different latitudes, so $g(\theta)$ has to be positive or negative for the corresponding latitude, as does $f(\theta)$. This means the production and loss rates could change sign from latitude to latitude, which is less realistic. Mathematically we can still solve $\chi(\theta,\xi)$. In principle, for each given r (and thus A_1 and $f(\theta)$), there might exist an analytical solution for $A(\theta,\xi)$. On the other hand, the only r term in the solution of $K(\theta,\xi)$ will be in the form $(e^{-\xi}\psi)^r$ and therefore can be absorbed in the $G(e^{-\xi}\psi)$ in $\chi(\theta,\xi,G)$. The analytic solution from Shia et al. (1990) corresponds to the situation that $r = 0$ and $g(\theta) = f(\theta)$. For $r \neq 0$, it might end up with a solution containing exponential integral functions.
2. Now we focus on the other possibility that the production and loss rates do not change sign at any latitude. We assume $(d\ln(A_2)/d\xi) = r(d\ln(e^{-\xi}\psi_2)/d\xi)$, so we have $A_2 = k(e^{-\xi}\psi_2)^r$. In order to solve for A_1, we need to diminish the ξ terms in the production and loss terms, i.e., both $e^{(\beta-1)\xi}/(d(e^{-\xi}\psi_2)/d\xi)$ and $e^{\alpha\xi}/(k(e^{-\xi}\psi_2)^r d(e^{-\xi}\psi_2)/d\xi)$ are constants. Note that $d(e^{-\xi}\psi_2)/d\xi$ is the altitudinal dependence of the horizontal velocity. For a fully closed stream function, for example, the air rises from the equator, flows to the polar region in the upper stratosphere, sinks at the poles and returns to the equator in the lower stratosphere, so the horizontal velocity has to change sign with altitude. Therefore, the production and loss terms would change sign with altitude accordingly. This is also less realistic. However, if we choose to only study part of the stratosphere, this is still useful for analyzing the behavior of the system. For simplicity, we let $\psi_2(\xi) = e^{\eta\xi}$, $\beta = \eta$,

and $\alpha = (r+1)(\eta-1)$. Therefore, for each given r (and thus α), there might exist an analytical solution for $A(\theta, \xi)$. The ODE is

$$\frac{dA_1}{d\theta} - \left(\frac{rd\ln(\psi_1)}{d\theta} + \frac{L_0 aHg(\theta)\cos\theta}{(\eta-1)\psi_1}\right) A_1 + \frac{P_0 aHf(\theta)\cos\theta}{k(\eta-1)\psi_1} = 0. \quad \text{(A6)}$$

If we define

$$X(\theta) = \frac{P_0 aHf(\theta)\cos\theta}{k(\eta-1)\psi_1}, \quad \text{(A7)}$$

$$Y(\theta) = \frac{rd\ln(\psi_1)}{d\theta} + \frac{L_0 aHg(\theta)\cos\theta}{(\eta-1)\psi_1}. \quad \text{(A8)}$$

The solution is

$$A_1(\theta) = e^{\int Y d\theta}\left[C_1 - \int Xe^{-\int Y d\theta} d\theta\right], \quad \text{(A9)}$$

and similarly,

$$K_1(\theta) = C_2 e^{\int Y d\theta}. \quad \text{(A10)}$$

The integral $\int Xe^{-\int Y d\theta} d\theta$ has a very strict requirement. We now discuss two typical stream functions.

1. Imagine an axis-symmetric equator-to-pole circulation pattern in each hemisphere. We introduced a simple stream function $\psi(\theta, \xi) = aw_0 e^{\eta\xi}\sin\theta\cos^2\theta$, so $w(\theta, \xi) = w_0 e^{\eta\xi}(\cos^2\theta - 2\sin^2\theta)$, and $v(\theta, \xi) = ((1-\lambda)aw_0 e^{\eta\xi}/H)\sin\theta\cos\theta$. The air rises from the equator and sinks at the poles in the upper part of the circulation ($\eta < 1$) and is reversed in the lower part ($\eta > 1$). Although we cannot find a way to unify the whole circulation pattern, the two branches could share the same form of the solution. We assume $g(\theta) = \sin^2\theta$, so that

$$Y(\theta) = \frac{rd\ln(\psi_1)}{d\theta} + \frac{L_0 H\sin\theta}{(\eta-1)w_0\cos\theta}, \quad \text{(A11)}$$

and therefore we have

$$e^{\int Y d\theta} = (\cos\theta)^{\frac{-L_0 H}{(\eta-1)w_0}}\psi_1^r. \quad \text{(A12)}$$

For simplicity we take $r = -1$ (so that $\alpha = 0$) and $f(\theta) = (\cos\theta)^{(-L_0 H/((\eta-1)w_0))}$, so that

$$\int Xe^{-\int Y d\theta} d\theta = \int \frac{P_0 aH\cos\theta}{k(\eta-1)} d\theta = \frac{P_0 aH\sin\theta}{k(\eta-1)}, \quad \text{(A13)}$$

and

$$A_1(\theta) = \frac{(\cos\theta)^{\frac{-L_0 H}{(\eta-1)w_0}}}{aw_0\sin\theta\cos^2\theta}\left[C_1 - \frac{P_0 aH\sin\theta}{k(\eta-1)}\right], \quad \text{(A14)}$$

$$A_2(\xi) = ke^{(1-\eta)\xi}. \quad \text{(A15)}$$

Similarly, we obtain $K(\theta, \xi)$ for any given r:

$$K(\theta, \xi) = C_2(\cos\theta)^{\frac{-L_0 H}{(\eta-1)w_0}}(e^{-\xi}\psi)^r. \quad \text{(A16)}$$

The only r term in the solution of $K(\theta, \xi)$ is in the form $(e^{-\xi}\psi)^r$ and therefore can be absorbed into $G(e^{-\xi}\psi)$ in $\chi(\theta, \xi, G)$.

Therefore, for the stream function given by $\psi(\theta, \xi) = aw_0 e^{\eta\xi}\sin\theta\cos^2\theta$, with a production rate $P(\theta, \xi) = P_0 N_0(\cos\theta)^{(-L_0 H/(\eta-1)w_0)}$, and a loss rate $L(\theta, \xi) = L_0 N_0 e^{(\eta-1)\xi}\sin^2\theta\chi$, the final solution for $\chi(\theta, \xi)$ is

$$\chi(\theta, \xi) = (\cos\theta)^{\frac{-L_0 H}{(\eta-1)w_0}}\left[G(e^{-\xi}\psi) - \frac{P_0 aH\sin\theta}{(\eta-1)e^{-\xi}\psi}\right]. \quad \text{(A17)}$$

2. Imagine the air rises from the south pole and sinks at the north pole in the upper atmosphere and returns to the south pole in the lower atmosphere. The stream function may look like $\psi(\theta, \xi) = aw_0 e^{\eta\xi}\cos^2\theta$, so $w(\theta, \xi) = -2w_0 e^{\eta\xi}\sin\theta$, and $v(\theta, \xi) = ((\lambda-1)aw_0 e^{\eta\xi}/H)\cos\theta$. As shown in (1), the same form of solution applies to the upper part of the circulation ($\eta < 1$) and the lower part ($\eta > 1$). We assume $g(\theta) = 1$, so that

$$Y(\theta) = \frac{rd\ln(\psi_1)}{d\theta} + \frac{L_0 H}{(\eta-1)w_0\cos\theta}, \quad \text{(A18)}$$

and we obtain

$$e^{\int Y d\theta} = \left(\frac{1+\sin\theta}{1-\sin\theta}\right)^{\frac{L_0 H}{2(\eta-1)w_0}}\psi_1^r. \quad \text{(A19)}$$

Again, we take $r = -1$ (so that $\alpha = 0$) and $f(\theta) = (1+\sin\theta/1-\sin\theta)^{(L_0 H/2(\eta-1)w_0)}$, so that

$$\int Xe^{-\int Y d\theta} d\theta = \int \frac{P_0 aH\cos\theta}{k(\eta-1)} d\theta = \frac{P_0 aH\sin\theta}{k(\eta-1)}, \quad \text{(A20)}$$

and

$$A_1(\theta) = \frac{\left(\frac{1+\sin\theta}{1-\sin\theta}\right)^{\frac{L_0 H}{2(\eta-1)w_0}}}{aw_0\cos^2\theta}\left[C_1 - \frac{P_0 aH\sin\theta}{k(\eta-1)}\right], \quad \text{(A21)}$$

$$A_2(\xi) = ke^{(1-\eta)\xi}. \quad \text{(A22)}$$

Similarly, we obtain $K(\theta, \xi)$ for any given r:

$$K(\theta, \xi) = C_2\left(\frac{1+\sin\theta}{1-\sin\theta}\right)^{\frac{L_0 H}{2(\eta-1)w_0}}(e^{-\xi}\psi)^r. \quad \text{(A23)}$$

The only r term in the solution of $K(\theta, \xi)$ is in the form $(e^{-\xi}\psi)^r$ and can be absorbed into $G(e^{-\xi}\psi)$ in $\chi(\theta, \xi, G)$.

Therefore, for the stream function given by $\psi(\theta, \xi) = aw_0 e^{\eta\xi}\cos^2\theta$, with a production rate $P(\theta, \xi) = P_0 N_0((1+\sin\theta)/(1-\sin\theta))^{(L_0 H/2(\eta-1)w_0)}$, and a loss rate $L(\theta, \xi) = L_0 N_0 e^{(\eta-1)\xi}\chi$, the final solution for $\chi(\theta, \xi)$ is

$$\chi(\theta, \xi) = \left(\frac{1+\sin\theta}{1-\sin\theta}\right)^{\frac{L_0 H}{2(\eta-1)w_0}}\left[G(e^{-\xi}\psi) - \frac{P_0 aH\sin\theta}{(\eta-1)e^{-\xi}\psi}\right]. \quad \text{(A24)}$$

APPENDIX B

SOLUTIONS FOR THE PURE DIFFUSIVE CASES

Ignoring the advection terms, the 2D diffusion equation is shown in Equation (12). Note that the equation $(\partial/\partial\xi)(K_0 e^{(\gamma-1)\xi}(d\chi/d\xi)) = 0$ has a solution like $\chi(\xi) = C_1 + C_2 e^{(1-\gamma)\xi}$. Therefore, if we further assume that

the solution of Equation (12) can be expressed as $\chi(\theta,\xi) = A(\theta)G(\xi)$, and $G(\xi) = C_1 e^{(1-\gamma)\xi}$, then the equation will be reduced to

$$\frac{G(\xi)}{a^2\cos\theta}\frac{d}{d\theta}\left(\cos\theta K_{yy}\frac{dA(\theta)}{d\theta}\right) + P_0 e^{(\alpha+1)\xi} f(\theta) - L_0 e^{\beta\xi} g(\theta)A(\theta)G(\xi) = 0. \quad \text{(B1)}$$

Taking $\alpha = -\gamma$, $\beta = 0$, and $x = \sin\theta$, we obtain

$$(1-x^2)\frac{d^2A}{dx^2} - 2x\frac{dA}{dx} + \frac{a^2P_0}{K_{yy}C_1}f(1-x^2) - \frac{a^2L_0}{K_{yy}}g(1-x^2)A = 0. \quad \text{(B2)}$$

Here we consider two cases:

1. With a constant production and a linear loss rate, i.e., $f(1-x^2) = 1$ and $g(1-x^2) = 1$, the equation reduces to the Legendre equation, and the solution is

$$\chi(\theta,\xi) = e^{(1-\gamma)\xi}\left(C_1 P_\nu(\sin\theta) + C_2 Q_\nu(\sin\theta) + \frac{P_0}{L_0}\right), \quad \text{(B3)}$$

where $P_\nu(\sin\theta)$ and $Q_\nu(\sin\theta)$ are Generalized Legendre functions with a negative non-integer $\nu = \sqrt{(1-4a^2L_0)/(K_{yy}-1)}/2$. In order to get real solutions, we require that $K_{yy}/a^2 > 4L_0$, i.e., the horizontal transport is faster than the loss processes.

In principle, we should have a symmetric solution in this symmetric system, i.e., $C_1P_\nu(\sin\theta) + C_2Q_\nu(\sin\theta) = C_1P_\nu(-\sin\theta) + C_2Q_\nu(-\sin\theta)$. Using the equality $P_\nu(-x) = P_\nu(x)\cos\pi\nu - 2\pi^{-1}Q_\nu(x)\sin\pi\nu$ (Polyanin & Zaitsev 2002), we obtain $C_2/C_1 = -2\pi^{-1}\tan(\pi\nu/2)$, so that

$$\chi(\theta,\xi) = C_1 e^{(1-\gamma)\xi} \times\left[P_\nu(\sin\theta) - \frac{2}{\pi}\tan\left(\frac{\pi\nu}{2}\right)Q_\nu(\sin\theta) + \frac{P_0}{C_1L_0}\right]. \quad \text{(B4)}$$

$C_1 = 0$ leads to a trivial case with a constant mixing ratio with latitude. If $C_1 \neq 0$, Equation (B4) will end up with a horizontal diffusive equilibrium solution.

2. Without chemical loss, but with a production rate $f(1-x^2) = (1-x^2)^n$, where $n = 0, 1, 2, 3\ldots$, Equation (B2) becomes

$$(1-x^2)\frac{d^2A}{dx^2} - 2x\frac{dA}{dx} + \frac{a^2P_0}{K_{yy}C_1}(1-x^2)^n = 0. \quad \text{(B5)}$$

If $n = 0$, i.e., with a constant production rate, the solution is

$$\chi(\theta,\xi) = C_1 e^{(1-\gamma)\xi}\left[C_2 + \frac{a^2P_0}{2K_{yy}C_1}\ln(\cos^2\theta) + \frac{C_3}{2}\ln\left(\frac{1-\sin\theta}{1+\sin\theta}\right)\right]. \quad \text{(B6)}$$

If $n = 1$, i.e., $f(1-x^2) = \cos^2\theta$, the solution is

$$\chi(\theta,\xi) = C_1 e^{(1-\gamma)\xi}\left\{C_2 + \frac{a^2P_0}{6K_{yy}C_1}[-\sin^2\theta + 2\ln(\cos^2\theta)] + \frac{C_3}{2}\ln\left(\frac{1-\sin\theta}{1+\sin\theta}\right)\right\}. \quad \text{(B7)}$$

Since the solutions should be symmetric about the equator, we should ignore the C_3 terms on the right-hand side. The solutions are

$$\chi(\theta,\xi) = \left[C_1 + \frac{a^2P_0}{2K_{yy}}\ln(\cos^2\theta)\right]e^{(1-\gamma)\xi}(n=0), \quad \text{(B8)}$$

and

$$\chi(\theta,\xi) = \left\{C_1 + \frac{a^2P_0}{6K_{yy}}[-\sin^2\theta + 2\ln(\cos^2\theta)]\right\} \times e^{(1-\gamma)\xi}(n=1). \quad \text{(B9)}$$

If the production rate peaks at the poles, e.g., $f(1-x^2) = x^{2n} = \sin^{2n}\theta$, Equation (B2) becomes

$$(1-x^2)\frac{d^2A}{dx^2} - 2x\frac{dA}{dx} + \frac{a^2P_0}{K_{yy}C_1}x^{2n} = 0. \quad \text{(B10)}$$

For $n = 1$, the solution is

$$\chi(\theta,\xi) = \left\{C_1 + \frac{a^2P_0}{6K_{yy}}[\sin^2\theta + \ln(\cos^2\theta)]\right\}e^{(1-\gamma)\xi}. \quad \text{(B11)}$$

REFERENCES

Allen, M., Yung, Y. L., & Waters, J. W. 1981, JGR, 86, 3617
Andrews, D. G., Holton, J. R., & Leovy, C. B. 1987, Middle Atmosphere Dynamics (New York: Academic)
Chamberlain, T. P., & Hunten, D. M. 1987, Theory of Planetary Atmospheres: An Introduction to Their Physics and Chemistry (New York: Academic)
Conrath, B. J., Gierasch, P. J., & Leroy, S. S. 1990, Icar, 83, 255
Friedson, A. J., West, R. A., Hronek, A. K., Larsen, N. A., & Dalal, N. 1999, Icar, 138, 141
Gladstone, G. R., Allen, M., & Yung, Y. 1996, Icar, 119, 1
Knutson, H. A., Charbonneau, D., Allen, L. E., et al. 2007, Natur, 447, 183
Lellouch, E., Bézard, B., Strobel, D., et al. 2006, Icarus, 184, 478
Liang, M. C., Shia, R. L., Lee, A. Y. T., et al. 2005, ApJL, 635, L177
Lin, J. S., & Hildemann, L. M. 1997, Atmos. Environ., 31, 59
Lindzen, R. S. 1981, JGR, 86, 9707
Moses, J., Fouchet, T., Bézard, B., et al. 2005, JGR, 110, E08001
Nixon, C. A., Achterberg, R. K., Conrath, B. J., et al. 2007, Icar, 188, 47
Nixon, C. A., Achterberg, R. K., Romani, P. N., et al. 2010, P&SS, 58, 1667
Polyanin, A. D., & Zaitsev, V. F. 2002, Handbook of Exact Solutions for Ordinary Differential Equations (London: Chapman & Hall)
Prather, M. J. 1986, JGR, 91, 6671
Shia, R., Ha, Y. L., Wen, J. S., & Yung, Y. L. 1990, JGR, 95, 7467
Strobel, D. 1974, ApJL, 192, L47
West, R., Friedson, A., & Appleby, J. 1992, Icar, 100, 245
Yelle, R. V., Griffith, C. A., & Young, L. A. 2001, Icar, 152, 331
Zhang, X. 2012, PhD Thesis, California Institute of Technology
Zhang, X., Nixon, C. A., Shia, R. L., et al. 2013, P&SS, submitted